DOI 10.1515/bmt-2013-0053 — Biomed Tech 2013; x(x): xxx–xxx

Short communication

Q1: Please check and confirm addition of "the" before Fuhrman grading system in the title

Michal Kruk, Stanislaw Osowski*, Tomasz Markiewicz, Wojciech Kozlowski, Robert Koktysz, Janina Slodkowska and Bartosz Swiderski

Nucleolus detection in the Fuhrman grading system for application in CCRC

Abstract: The paper presents a method for nucleolus detection in images of nuclei in clear-cell renal carcinoma (CCRC). The method is based on the similarity of the nuclei image and the two-dimensional paraboloidal window function. The results of numerical experiments performed on almost 2600 images of CCRC nuclei have confirmed the good accuracy of the method. The developed algorithm will be used to accelerate further research in computer-assisted diagnosis of CCRC.

Keywords: Fuhrman grading; renal carcinoma cells; image processing; nucleolus detection.

***Corresponding author: Stanislaw Osowski,** Warsaw University of Technology, ul. Koszykowa 75, Warsaw, Poland; and Military University of Technology, Kaliskiego 2, 00-908 Warsaw, Poland, Phone: +48-22-234-7235, Fax: +48-22-234-5642, e-mail: sto@iem.pw.edu.pl
Michal Kruk and Bartosz Swiderski: Warsaw University of Life Sciences, Nowoursynowska 166, 02-787 Warsaw, Poland
Tomasz Markiewicz: Warsaw University of Technology, ul. Koszykowa 75, 00-661 Warsaw, Poland; and Military Institute of Medicine, Szaserów 128, 04-141 Warsaw, Poland
Wojciech Kozlowski, Robert Koktysz and Janina Slodkowska: Military Institute of Medicine, Szaserów 128, 04-141 Warsaw, Poland

An important step in the research on clear-cell renal carcinoma (CCRC) is recognition of tumor cells [2, 3, 6]. Tumor cells are generally large and polygonal and show distinct cell membranes. The cytoplasm is optically clear in most cells; hence the analysis is simplified to their nuclei. The nuclei are small, round to slightly oval, and regular. They can be recognized on the basis of the existence of one of even a few nucleoli.

Analysis of the image directed to the recognition of nuclei is the first step in the assessment of the degree of advancement of a cancer by applying the Fuhrman grading system composed of four grades [3]. Grade 1 tumors have round, uniform nuclei with invisible or absent nucleoli. Nuclear contours at grade 2 are more irregular than those at grade 1, and nuclei of about 15 μm in diameter are well visible at high magnification with existing nucleoli. At grade 3, the nuclear contours are even more irregular in size and shape and reach diameters of about 20 μm and the nucleoli are well visible. The size of cells of grade 4 exceeds 20 μm. The nuclei are pleomorphic and hyperchromatic with hardly visible or absent nucleoli.

Q2: The description of Fuhrman was not clear. It was not mentioned whether the nucleoli are visible or invisible at this magnification. The copy editor assumed the former. Please check

The simplest methods for assessing Fuhrman grade in CCRC are based on the observation of nucleoli at different magnifications. If nucleoli are invisible even at magnification equal to 400×, it they are classified as Fuhrman 1; if they are visible at magnification equal to 200×, they are classified as Fuhrman 2; and if they are visible at magnification of 100×, they are classified as Fuhrman 3 [6]. At grade 4, the nucleoli are seldom observed, and the most visible sign of this stage is the existence of clumped chromatin.

Therefore the problem of nucleoli detection is very important in CCRC research. However, we should be aware that the final determination of Fuhrman grade usually also takes into account other factors characterizing the nuclei, like the size, regularity, texture, geometrical parameters, histogram, etc. All of them form a more complex set of features used in determination of Fuhrman grade. This paper is devoted only to the detection of nucleoli.

Manual detection of nucleoli under a microscope by a pathologist is error prone due to the subjective perception of humans. In fact, the same pathologist might differ in the detection and classification of the same cell nuclei within the same image in a second annotation round. The reasons for such a discrepancy may relate to the fuzzy distribution of colors in the nuclei, the heterogeneity of nuclear features in the same tumor, the partial destruction of a cell nucleus and the subjective experiences of the pathologist. Therefore, decisions for grading a cancer may be inconsistent among pathologists.

The automatic computer-based recognition of nuclei and nucleoli in a CCRC may represent a good remedy for such a problem. However, it represents a challenging, still unsolved task for researchers. The complexity of the data, as well as the intensive laboratory practice needed to obtain them, makes the development of such automatic tools very difficult.

In this paper, we consider an automated processing pipeline for the detection of nucleoli in images of the nuclei in CCRC. The procedure consists of several consecutive tasks, which can be mapped to machine learning challenges. To get satisfactory results with the nuclei extraction, we have to solve different sub-tasks of image processing by applying a mathematical morphology (erosion, dilation, closing and opening), Gaussian filtering, gradient operators for edge detection, different types of color-based operations and, finally, the watershed algorithm to separate the glued nuclei. The segmented nuclei data saved in a file are subjected to further processing, leading finally to the detection of nucleolus present in the nucleus. The last task will be the main subject of this paper. The results of this research represent an important part of our work directed at describing the morphological features of nuclei and nucleoli in CCRC, leading finally to the evaluation of Fuhrman grade on the basis of histological images of renal tissues.

The segmentation of nuclei from a slide of CCRC requires performing a few steps. After reading the original image in RGB format, smoothing is needed, which means removal of small particles that disturb the image. This operation is implemented in three steps: histogram equalization which enhances the contrast of the image by transforming the values of pixel intensity for better visibility of chromatin structure, morphological erosion (at circular structural element of 5 pixels in size) and, finally, application of a Gaussian filter [4, 9]. After all these operations, we obtain a smoothened image, ready for further processing.

The next step is edge detection which is the crucial part of nuclei segmentation. To counteract the different luminosities of some parts of the image arising from hematoxylin and eosin staining, we solved the edge detection problem by using a gradient method, instead of the often used automatic thresholding [1, 5, 8]. We found that the discrimination function of the gradient is significantly resistant to the noise of the background.

After the edge detection, the binary mask representing the nuclei discovered in the image is prepared. It is obtained through the morphological operations of closing and opening using the structural element of the disk shape and size equal to 3. These operations allow to avoid the disturbances on the circumference of the nucleus. The mask is then multiplied by the original image and, as a result, we obtain the nucleus without edge disturbances. In the following step, Gaussian filtering of the nucleus image is applied. It helps to smoothen the image by eliminating small local minima and maxima representing some irregularity in color distribution.

In an automatic nuclei extraction process, the structures not representing the nuclei may also be extracted.

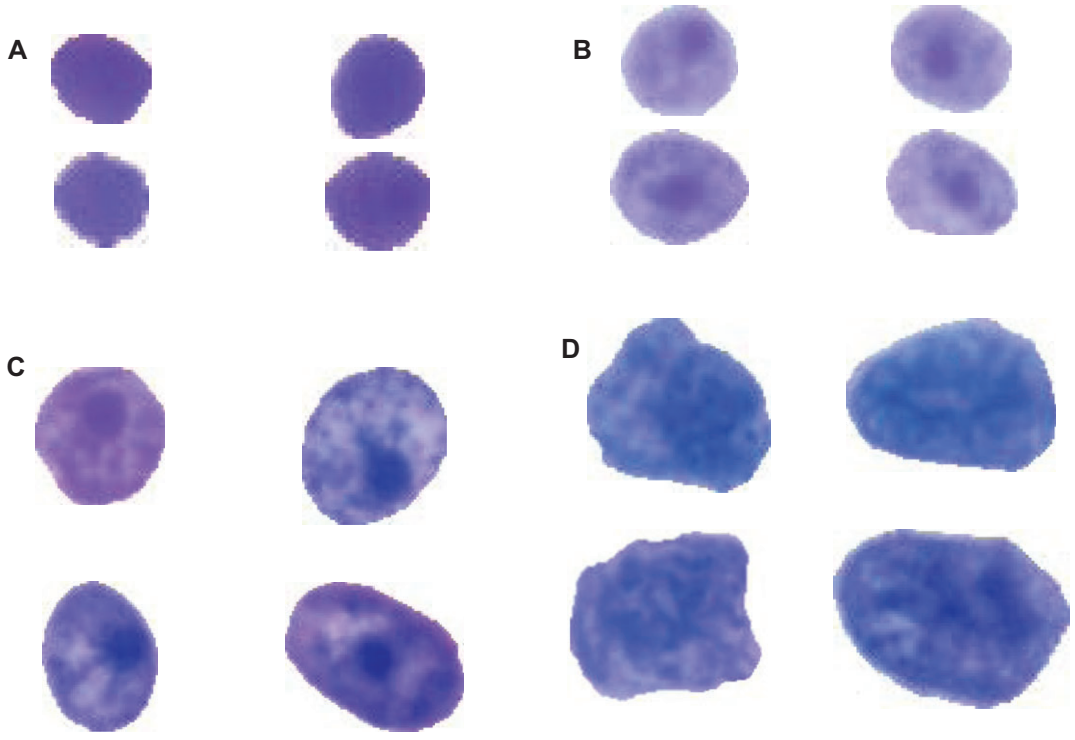

Figure 1 Typical examples of different grades of the nuclei of CCRC: (A) grade 1, (B) grade 2, (C) grade 3 and (D) grade 4.

For the nuclei, we treat only the structures described by similar shape factors which may slightly differ from the circular shape. Therefore any segmented structure must go through the test of circularity. We estimate the major and minor axis of each structure. The extracted structure is accepted as a nucleus if the ratio between its major and minor axis does not exceed the value of 1.5. After the image is segmented, all nuclei data are saved to a file as separate objects for further processing.

All numerical experiments were performed by using the base of histological images of CCRC representing different Fuhrman grades, collected from the archive of the Warsaw Military Institute of Medicine and annotated by medical experts. The images represent microscopic images with a magnification of 400× and a resolution of 2070×1548 and are saved in Tiff format. Almost 2600 nuclei were automatically segmented using the presented procedure. Examples of automatically segmented nuclei, corresponding to different Fuhrman grades, are shown in Figure 1.

The images are presented in a scale preserving as much as possible the proportion of the sizes of different grades of the nuclei. The representatives of each grade differ by size, texture, presence or absence of the nucleoli, details of color, homogeneity of the structure, etc.

As can be seen, there are no (or it is very hard to observe) nucleoli in the nuclei images representing grades 1 and 4. In grades 2 and 3, the nucleoli are well visible at a magnification of 400×. The size of the nucleoli with grades of 2 and 3 is also different. This fact can be used to create additional features in the process of recognition of the grades of the CCRC. In this paper, we concentrate on the method of finding the nucleoli.

After segmenting the nuclei from CCRC slides, the next step is to detect the presence of nucleoli in them. The nucleoli are of fuzzy nature, weakly differing from the nuclei background. Furthermore, several artifacts, such as clumped chromatin, may be falsely treated as the nucleoli. For these reasons, application of thresholding methods, for example, between-class variance of Otsu, Gaussian mixture modeling, minimum error thresholding [1, 5, 8], etc., results in an unacceptable misrecognition rate of nucleoli in the population of analyzed nuclei images.

The proposed approach to nucleoli detection uses the idea of correlation. Analyzing the three-dimensional (3-D) view of the images of the nuclei, we can see that the shape of the nucleolus resembles the paraboloid placed on the platform formed by the background of the nucleus.

Examples of the 3-D visualization of CCRC images of different grades are depicted in Figure 2. It is easy to observe that the 3-D images representing grade 1 are flat. Images of grades 2 and 3 containing visible nucleoli have characteristic hills of different sizes and shapes. The existence of a hill is very characteristic for the presence of nucleoli. Hence our method of discovering the nucleolus in the image uses the measure of similarity of the potential hills and paraboloids of different sizes located at different positions in the image. The highest measure of similarity is obtained for the location of paraboloid compatible with the nucleolus and for the size of paraboloid comparable to the size of the nucleolus. In this way, we get

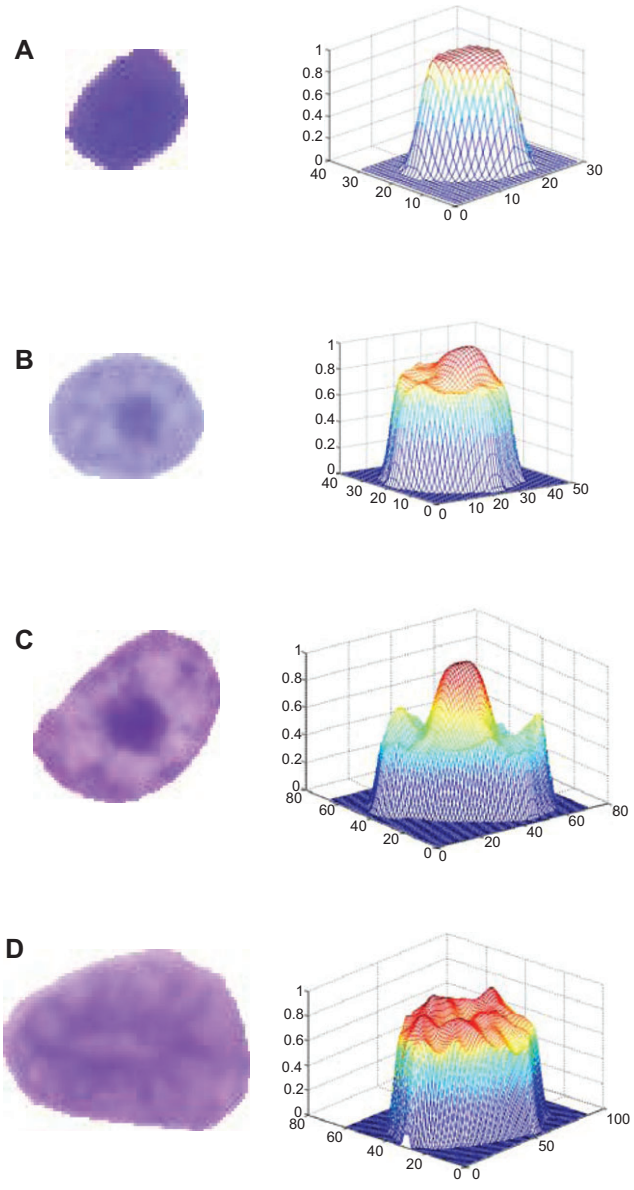

Figure 2 Typical examples of different grades of the nuclei of CCRC (left) and their 3-D views (right): (A) grade 1, (B) grade 2, (C) grade 3 and (D) grade 4.

Q3: Please indicate which study in the sentence "In general, researchers"

Q4: Please check and confirm that italic, Roman and bold have been applied correctly in text and equations throughout

the information for both the location and the size of the nucleolus.

In the images of grade 4, the clumped chromatin is well visible and this is reflected on the 3-D plot [7] as a hilly landscape with many low-height hummocks with heights much smaller than those found in images of grades 2 and 3. In general, researchers agree that nuclei images of grade 4 CCRC contain no nucleoli.

The general procedure of nucleoli detection is presented in Figure 3. After reading the segmented image of the nuclei, the first step of processing is image normalization. The intensity of pixel at any (x,y) position of the image is normalized by using the following equation:

$$L'(x,y)=\frac{L(xy)-\min(L)}{\max(L)-\min(L)} \tag{1}$$

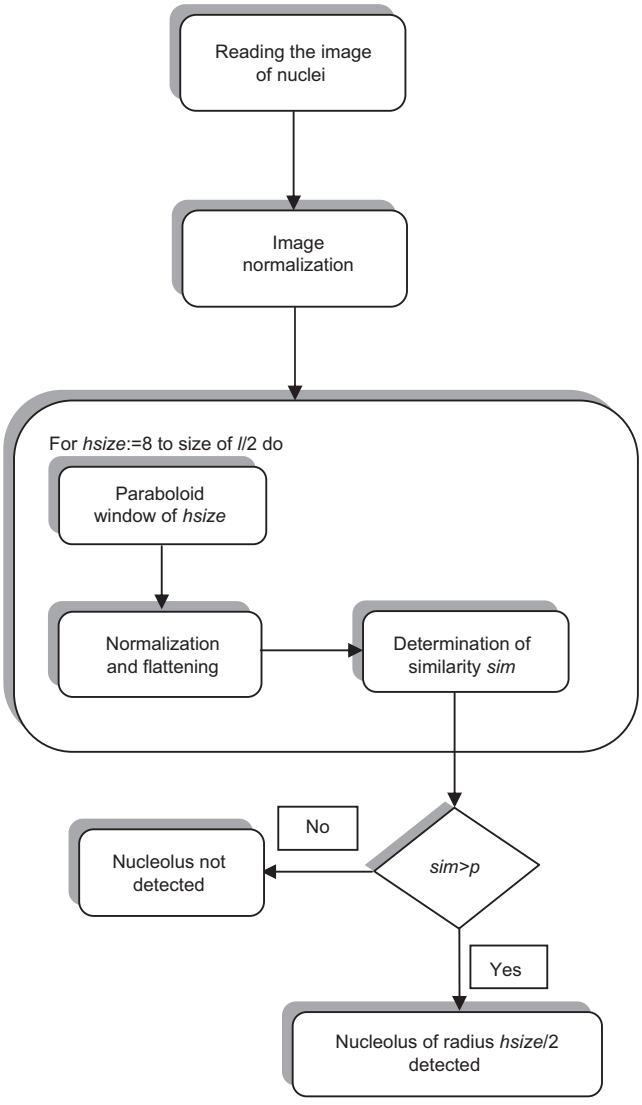

Figure 3 Diagram of the procedure leading to the detection of nucleoli.

where $L'(x,y)$ and $L(x,y)$ are, respectively, the normalized and original values of pixel intensity at position (x,y), and max and min represent, respectively, the highest and lowest values of pixel intensities in the original image.

In the next step, the paraboloid window **H** in 2-D space (x and y coordinates) is generated. It is described by the following equation

$$H(x,y)=-\left(\frac{x^2}{2}+\frac{y^2}{2}\right) \tag{2}$$

The size of window **H** (called *hsize*) represents the dimension of the square within which the values of $H(x,y)$ are calculated. The size of **H** should be correlated with the size of the nucleolus. To determine its proper value, we have tried different values changing from the minimum *hsize* (equal to 8 pixels in experiments) to half of the nucleus size ($l/2$).

The paraboloid window is first normalized using the same equation (Equation 1) as in the original image. Then background flattening of the window is applied to make its 3-D shape resemble the shape of the intensity of the pixels in the nucleolus. The operation of flattening is done by using the following transformation

$$H(x,y):=\begin{cases} H(x,y) & \text{if} \quad H(x,y)\geq \text{mean}(\mathbf{I}) \\ \text{mean}(\mathbf{I}) & \text{if} \quad H(x,y)<\text{mean}(\mathbf{I}) \end{cases} \tag{3}$$

The result of the flattening performed on the paraboloid window after normalization and flattening is presented in Figure 4. Figure 4A depicts the normalized paraboloid and Figure 4B the shape of it after the flattening.

In our algorithm, the size *hsize* of window **H** is changed from the minimum value assumed as 8 to half of the nucleus image size. The lowest value corresponds to the minimum size of the nucleoli that has been observed in practice. The highest limit is based on the observation that the nucleoli size never exceeds half the size of the nuclei.

In the next step, we estimate the similarity between **H** and different subimages **I′** of the analyzed nuclei image with the central point of **I′** located in the i, jth position of the analyzed image for all possible values of i and j. This calculation is repeated for each value of *hsize* in association with the i, jth pixel treated as the central point of **I′** of the nucleus. The experiments with the similarity measure defined on the basis of the 2-D correlation function [7] did not lead to the satisfactory results of recognition. Hence we propose the following definition of similarity

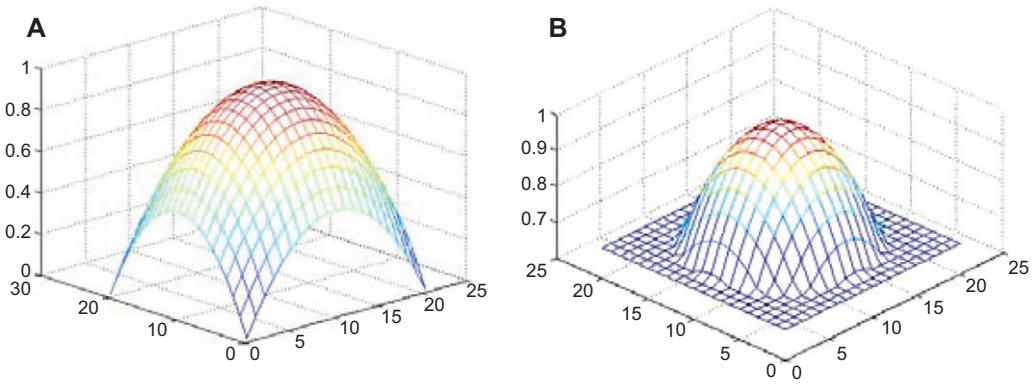

Figure 4 Normalized paraboloid visualization of size 21: (A) the original paraboloid and (B) paraboloid after "flattening".

$$sim(hsize, i, j) = 1 - \frac{\text{mean}(|H(x,y)^2 - I'(x,y)^2|)}{(1 - \text{mean}(I(x,y)))^2} \quad (4)$$

where *sim*(*hsize*, *i*, *j*) means the estimated similarity value dependent on the *hsize* and position of the central point of image **I′**. For each value of *hsize*, the maximum of the *sim* measure is determined. The highest value of *sim* at a particular location of *i* and *j* indicates that, in this location, the nucleolus can potentially exist. After checking all possible values of *hsize* as the optimal one, we selected this one, which provides the absolute maximum among all checked values.

We illustrate this process for two types of nuclei images: one containing the visible nucleolus and one without the nucleolus. Figure 5A depicts the case with the visible nucleolus. Its 3-D plot (Figure 5B) confirms this fact by the presence of a hill inside of the plot. Table 1 shows the change in similarity *sim* with the *hsize* parameter varying from the minimum to the maximum value. As the optimal size, we treat this one which provides the highest value of *sim* (in this case *hsize*=14). Figure 5C depicts the position and size (the encircled region) of the identified nucleolus.

The alternative case of an image containing no visible nucleolus is presented in Figure 6. The dependence of similarity measures on the value of *hsize* is presented in Table 2. This time the similarity parameter *sim* assumes low values, only slightly varying with the change in *hsize*. No visible maximum point of this relation significantly differing from the other values was observed.

An interesting comparison of the cases representing different Fuhrman grades of visible and nonvisible

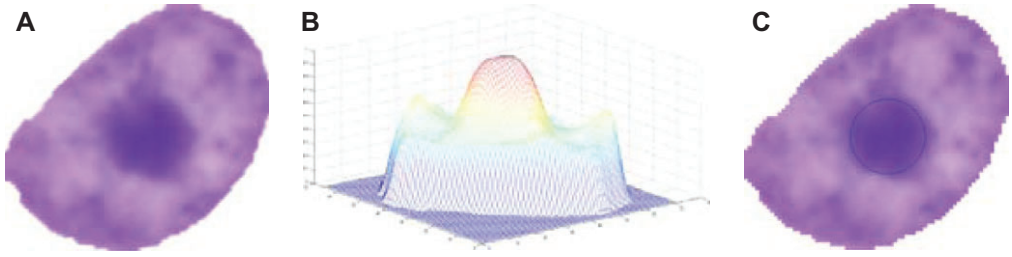

Q5: Please supply better quality figures. Figures 5 & 6

Figure 5 Example of nuclei with a visible nucleolus: (A) the original image of the nuclei, (B) its 3-D shape and (C) the discovered nucleolus denoted by a circle.

Q6: Please indicate the significance of the italic emphasis (or similarly bold) in Tables 1 and 3 as a footnote.

Table 1 Dependence of the *hsize* parameter and the similarity value in the case of visible nucleolus in the nucleus image.

sim	0.34	0.51	0.74	*0.88*	0.81	0.67	0.55	0.45	0.36	0.29	0.22	0.15
hsize	8	10	12	*14*	16	18	20	22	24	26	28	30

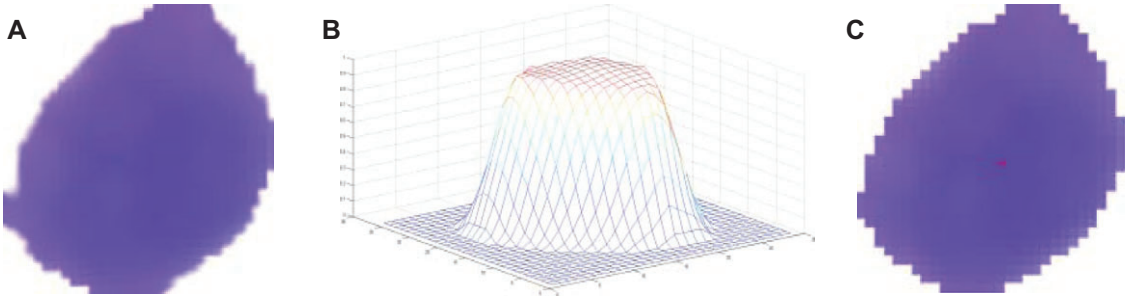

Figure 6 Example of nuclei without a visible nucleolus: (A) the original image of the nuclei, (B) its 3-D shape and (C) a graphical representation of the recognition – the red point indicates only the darkest region; no nucleolus was discovered.

Table 2 Change in similarity value for different values of the *hsize* parameter in the case of no visible nucleolus in the nucleus image.

sim	0.12	0.14	0.16	0.22	0.31	0.34	0.31	0.24	0.16	0.07	0.07	0.06
hsize	8	9	10	11	12	13	14	15	16	17	18	19

nucleoli is presented in graphical form in Figure 7. As can be seen, the distribution of similarity values differs for all grades. We can observe a great change in the similarity measure for the images with well-visible nucleolus (grades 2 and 3). In the case of images (grades 1 and 4) with no visible nucleolus, the similarity measure is relatively insensitive to the change in *hsize* and assumes significantly lower absolute values of *sim*.

An important step is how to determine the optimal similarity threshold value that allows to recognize the

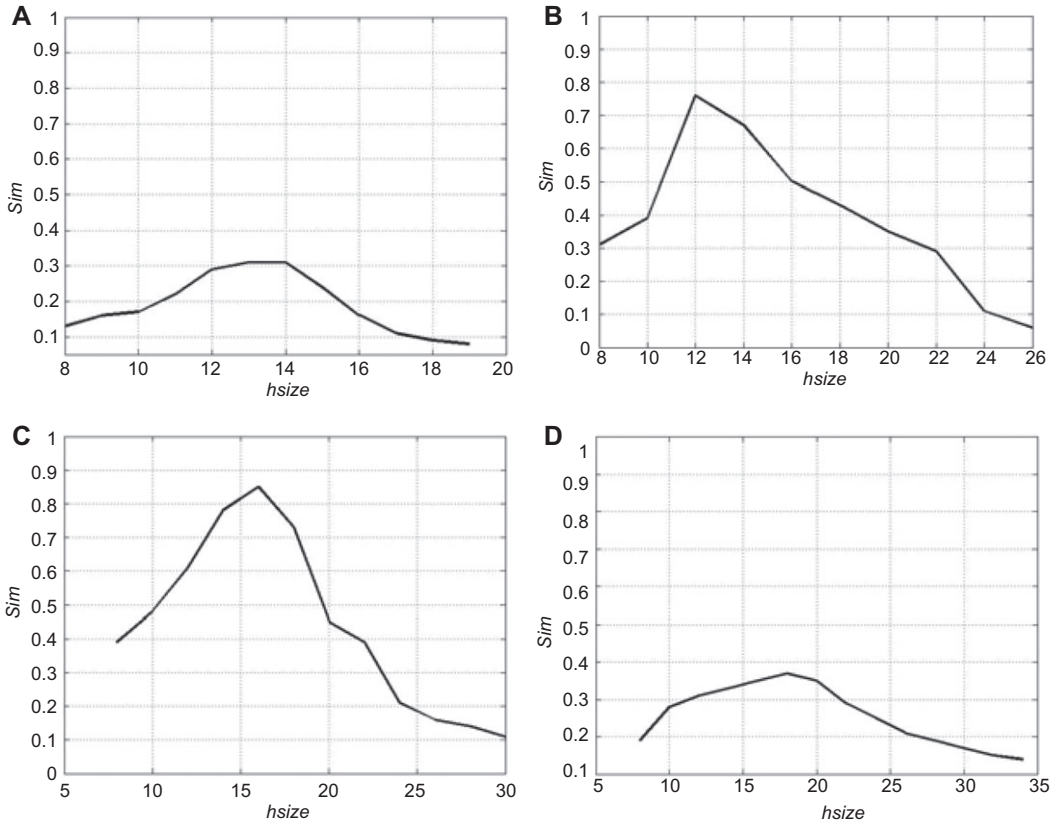

Figure 7 Dependence of the *sim* measure versus *hsize* for the images representing different Fuhrman grades: (A) grade 1, (B) grade 2, (C) grade 3 and (D) grade 4.

Table 3 Results of nucleoli detection with changing threshold value of *sim*.

sim threshold	0.1	0.2	0.3	0.4	*0.5*	0.6	0.7	0.8	0.9	1	Expert score
Without nucleolus	1618	1618	1614	1602	*1598*	1398	1242	1090	960	848	1618
With nucleolus	0	128	366	682	*878*	880	902	932	956	970	970
Relative error, %	37.48	32.53	23.49	11.75	*4.33*	11.98	17.16	21.87	25.97	29.75	–

The minimum relative error was around the *sim threshold* equal to 0.5. To confirm this result, we calculated this error at a much smaller step size (equal 0.01), around the estimated optimal value. The results of these experiments are presented in Table 4.

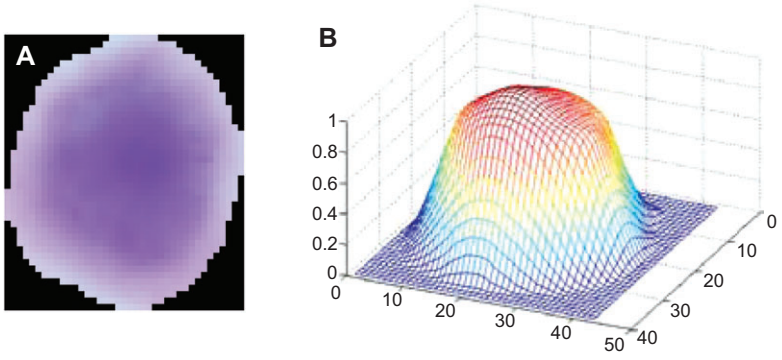

Figure 8 A nucleus image with a hardly visible nucleolus (A) and its 3-D shape (B).

existence of nucleolus in the image of nuclei. We have done it in an experimental way by trying different values of *sim* threshold on the set of available images of the nuclei. The threshold value providing the best fit of an automatic recognition of nucleoli to the results of a human expert is treated as the optimal one.

To obtain this value, we performed experiments which included all images of nuclei existing in our database with threshold values changing from 0.1 to 1 with a small step size. The total number of all nuclei images used in these experiments was equal to 2588. Table 3 depicts the statistical results, presenting the number of discovered nucleoli in the investigated set of images of the nuclei. Column 12 of Table 3 (denoted as the expert score) depicts the reference distribution of the population of the analyzed images. The analyzed base of images contained 970 cells with nucleoli and 1618 cells without nucleoli. These numbers, estimated by an expert, are treated as the reference. The results of the application of our approach to nucleoli identification at each threshold value, tried in experiments, are then compared to the expert results. The misrecognition rates are presented in the last row of the table. Row 2 shows the estimated number of nuclei images without nucleolus and row 3 shows the number of images with recognized nucleolus.

The most important sources of the misrecognition are the very high level of fuzziness of the nucleolus colors because of the stain applied to the cells and the great similarity to the background. A typical example of this difficulty is presented in Figure 8. According to the human expert, the existence of nucleolus in this image is dubious, although possible. The 3-D shape of it shows a very faint increase in the height corresponding to the position of the potential nucleolus. The actual maximum *sim* value in this case was below 0.3, and our algorithm treated this image as one without nucleolus.

Summarizing, the paper has presented a computerized automatic method for recognition of nucleoli in slide

Q8: The original text was not clear in the sentence "The most... backgro[illegible]" Please [illegible] whether the edited text is correct.

Q7: Please indicate the significance of [illegible] is. Indicate also which is the expert score in Table 4

Table 4 Relative error of nucleoli detection at reduced step size of the threshold value of *sim*.

sim threshold	0.45	0.46	0.47	0.48	0.49	*0.5*	0.51	0.52	0.53	0.54	0.55
Relative error, %	6.49	5.33	4.75	4.48	4.33	*4.33*	4.40	4.75	5.41	6.45	7.65

The last row of the table depicts the total relative error of recognition of the nucleoli at different values of the applied threshold, taking the expert score as the reference. As we can see, its lowest value equal to 4.33% corresponds to the similarity threshold values of 0.49 and 0.5. The value of 0.5 has been confirmed and it is treated as an optimal one.

images of clear-cell renal carcinoma (CCRC). The developed method explores the idea of 2-D correlation between a specially created paraboloidal window and an investigated nucleus image of CCRC. The experiments carried out on a set of a few thousand images show that the average nucleoli misrecognition rate is below 5%, and such level of error is acceptable in a biomedical image analysis. The developed algorithm will be used to accelerate research in computer-assisted diagnosis of CCRC.

Received May 8, 2013; accepted July 11, 2013

Q9: As per journal style references were re-numbered according to alpha-numerical order in and reference list. Please check & confirm

References

[1] Demirkaya O, Asyali MH, Sahoo PH. Image processing with MATLAB: applications in medicine and biology. Boca Raton, FL: CRC Press 2009.
[2] Finley D, Pantuck A, Belldegrun A. Tumor biology and prognostic factors in renal cell carcinoma. Oncologist 2011; 16(Suppl 2): 4–13.
[3] Fuhrman SA, Lasky LC, Limas C. Prognostic significance of morphologic parameters in renal cell carcinoma. Am J Surg Pathol 1982; 6: 655–663.
[4] Gonzalez R, Woods R. Digital image processing. Englewood Cliffs, NJ: Prentice Hall 2008.
[5] Kittler J, Illingworth J. Minimum error thresholding. Pattern Recogn 1986; 19: 41–47.
[6] Kontak JA, Campbell SC. Prognostic factors in renal cell carcinoma. Urol Clin North Am 2003; 30: 467–480.
[7] MatLab user manual – Image processing toolbox. Natick, MA: MathWorks 2012.
[8] Soille P. Morphological image analysis, principles and applications. Berlin: Springer 2003.
[9] Soille P, Otsu N. A threshold selection method from grey-level histograms. IEEE Trans Sys Man Cyber 1979; 9: 62–66.